Egyptian Geophysical Society
EGS Journal, vol. 3, No. 1, 35-40 (2005)

VERTICAL VELOCITIES IN THE KOREAN PENINSULA FROM PERMANENT GPS NETWORKS

Ahmed M. Hamdy[1,2]

(1) Korea Astronomy Observatory,61-1, Hwaam-dong, Yuseong-gu, Daejeon 305-348, South Korea.
(2) Geodynamics Department, National Research Institute of Astronomy and Geophysics, Helwan, Cairo, Egypt

السرعات الرأسية فى شبة الجزيرة الكورية باستخدام محطات الرصد الدائم لنظام الاحداثيات الشامل

الخلاصة: يعتبر الرصد الدائم باستخدام نظام الاحداثيات الشامل طريقة مهمة فى تحديد حركة القشرة الأرضية حيث له القدرة على تحديد هذه الحركات فى مدة زمنية أقل من المدة المطلوبة باستخدام الطرق التقليدية.

وباستخدام أرصاد ثلاث سنوات مجمعة من ٥٠ محطة رصد دائمة تم حساب السرعة الرأسية فى شبه الجزيرة الكورية. وعند تصحيح الأرصاد تم استخدام طريقة التصحيح المفيد وذلك لتقليل تأثير الموجة الشائعة التى وجدت بوضوح عند تطبيق نظام تحديد موقع النقطة الدقيقة. وتوضح النتائج التى تم الحصول عليها أن معدل السرعة الرأسية فى شبة الجزيرة الكورية حوالى ١,٣ مم/ سنة.

Abstract: *GPS on permanent stations has proved to be a powerful tool in crustal movement studies, capable to detect small trends of movement in a frication of time that required by the classical methods. Using three years data collected from fifty GPS permanent stations in South Korea the vertical velocity was determined. The constrained network adjustment technique was used in the adjustment step in-order to minimize the common mode signal effect, which is clearly found in the precise point positioning solutions. The obtained results show that the average vertical velocity in the Korean peninsula is 1.3 mm/year.*

INTRODUCTION

The levelling network in Korea was initially established by 1910-15, but the Korean War virtually destroyed all the existing marks in the Southern part of the Korean Peninsula. Since 1960, The National Geographic Information Institute of Korea (NGII) reconstructed the first order-levelling network and it was completed by 1986. This network composed of 16 loops and 38 routes with a total length of 3,400 km and 2,030 benchmarks spaced at 2-4 km while the primary benchmark of South Korea is suited at Inha University in the city of Inchon (Cho, 1999).

The precise surveying using Global Positioning System (GPS) in South Korea had been started by 1994, with the establishment of the first permanent GPS station at the Korea Astronomy Observatory campus (Park et al., 2001). Nowadays the total number of operating GPS permanent stations are more than seventy (Park et al., 2003). The active stations are deployed such that any point in South Korea will be within 30 km of the nearest active station.

Both repeated precise levelling and permanent GPS measurements provide estimates of vertical velocities with high formal precision. For modern levelling, precision estimates (one-sigma) are typically $0.8\,mm/\sqrt{km}$ or better (Mäkinen et al., 2003). Thus over a distance of 100 km (assuming white noise) two levellings at 40 years intervals would give velocity difference to better than 0.3 mm/year. In precise levelling network, redundancy in observations is provided by loop closures only, and in a single campaign the model is thus poorly controlled, as all errors do not necessarily appear in the misclosures. The situation is not better when we model vertical motion on the basis of two campaigns where any differences between them are absorbed into the motion model. Therefore in-order to have an accurate estimation for the vertical velocity from precise levelling observations we need nearly 80 years since the initial observation time, which is not available in our case as the Korean first order-levelling network was completed by 1986. Over the same distance (100 km) the scatter weekly GPS solutions of coordinate's differences in the vertical is around 3 mm. Then, and by considering the white noise, in less than 3 years of continuous GPS observations, the vertical velocity difference would be determined by accuracy better than 0.3 mm/year (Mäkinen et al., 2003). However, it is well known that such error estimates tend to be too optimistic, and the assessment of the accuracy quite difficult. GPS coordinates time series do not usually display white noise on top of linear trend. Changes in instrumentation, in environmental condition, and in the reference system may cause jumps. Even when this can be avoided, the noise tends to be red or brown and a number of periodic phenomena appear (Mao et al., 1999; Scherneck et al., 2002).

Since, the available repeated levelling observations are poorly controlled where hardly we have two levelling campaigns the vertical velocity in the Korean peninsula is determined by using all the available data from the Korean GPS Network (fig. 1).

Data Processing

The Korean GPS Network (KGN) consists of 50 stations two of them, DAEJ and SUWN, are International GPS Service (IGS) stations (Hamdy et al., 2004). The KGN was fully operated by 2000; all the stations have a dual-frequency receivers Trimbel 4000SSi while two different antenna types were used "TRM29659.00 and TRM 33429.00" (Table 1).

Table (1): Summary of the Korean Geodetic Network

Agency	Number of sites	GPS Receiver	GPS Antenna	IGS
KAO	9	Trimble 4000SSi	TRM 29659.00	DAEJ
MOGAHA	30	Trimble 4000SSi	TRM 33429.00	none
NGII	14	Trimble 4000SSi	TRM 29659.00	SUWN

Korea Astronomy Observatory (KAO).
Ministry of Government Administration and Home Affairs (MOGAHA).
National Geographic Information Institute (NGII).

We analyzed the KGN data from April 2000 to March 2003 by using Bernese Software Version 4.2 (Beutler et al., 2001). The used data in this study shows a clear common-mode signal in the vertical component as it was processed by GIPSY-OASIS software using the precise point positioning technique (Park et al ., 2003). Moreover their results show that, the common-mode signals from MOGAHA sites have somewhat different pattern from KAO and NGII. They claimed that the variation in the common-mode signals resulted from neglecting the antenna phase center corrections. In the processing step "KAO and NGII use the same antenna type, while MOGAHA sites use a different one".

In this study the IGS final orbits, the Satellite clock offset and Earth orientation parameters are used in data processing. The tropospheric delay was estimated by using GPSEST program and the QIF strategy is employed in the ambiguity resolution step. For the daily solutions, in-order to unify the common-mode signals (resulted from different antenna types) the antenna phase center had been corrected by using the standard models offered by the International GPS Service (IGS)

Table 2. Stations normal velocity and their RMS.

Station	E	N	Vertical	RMS	Station	E	N	Vertical	RMS
BHAO	128.98	36.16	0.08	0.21	MUJU	127.66	36.00	-1.20	0.16
CHCN	127.71	37.87	1.23	0.14	NAMW	127.40	35.42	-0.44	0.15
CHLW	127.42	38.16	-0.49	0.14	NONS	127.10	36.19	-2.61	0.16
CHNG	128.48	35.53	1.97	0.15	PAJU	126.74	37.75	1.71	0.15
CHYG	126.80	36.46	1.34	0.14	PUSN	129.07	35.23	0.12	0.14
CNJU	127.46	36.63	-3.27	0.18	SBAO	128.46	36.93	-2.29	0.38
DOND	127.06	37.90	2.62	0.14	SESO	126.49	36.78	-1.47	0.16
GOCH	127.94	35.67	1.27	0.14	SKCH	128.56	38.25	-0.03	0.13
GSAN	127.79	36.82	3.04	0.13	SKMA	126.92	37.49	0.35	0.23
HADG	127.71	35.16	-2.64	0.15	SNJU	128.14	36.38	-1.75	0.20
HONC	128.19	37.71	0.67	0.14	SONC	127.49	34.96	1.63	0.20
INCH	126.69	37.42	-0.14	0.14	SOUL	127.08	37.63	1.78	0.11
INJE	128.17	38.07	1.03	0.14	SUWN	127.05	37.28	1.65	0.12
JUNJ	127.14	35.84	1.36	0.12	TEGN	128.80	35.91	-0.75	0.12
KANR	128.87	37.77	-0.02	0.17	WNJU	127.95	37.34	0.74	0.14
KIMC	128.14	36.14	2.00	0.23	WOLS	129.42	35.51	-1.44	0.15
KUNW	128.57	36.23	0.67	0.14	YANP	127.51	37.45	-1.58	0.16
KWNJ	126.91	35.18	2.01	0.20	YECH	128.45	36.65	1.09	1.20
MKPO	126.38	34.82	0.45	0.16	YONK	126.52	35.28	-0.52	0.27
MLYN	128.74	35.49	0.12	0.28	YOWL	128.46	37.18	2.33	0.17

** DAEJ is fixed*

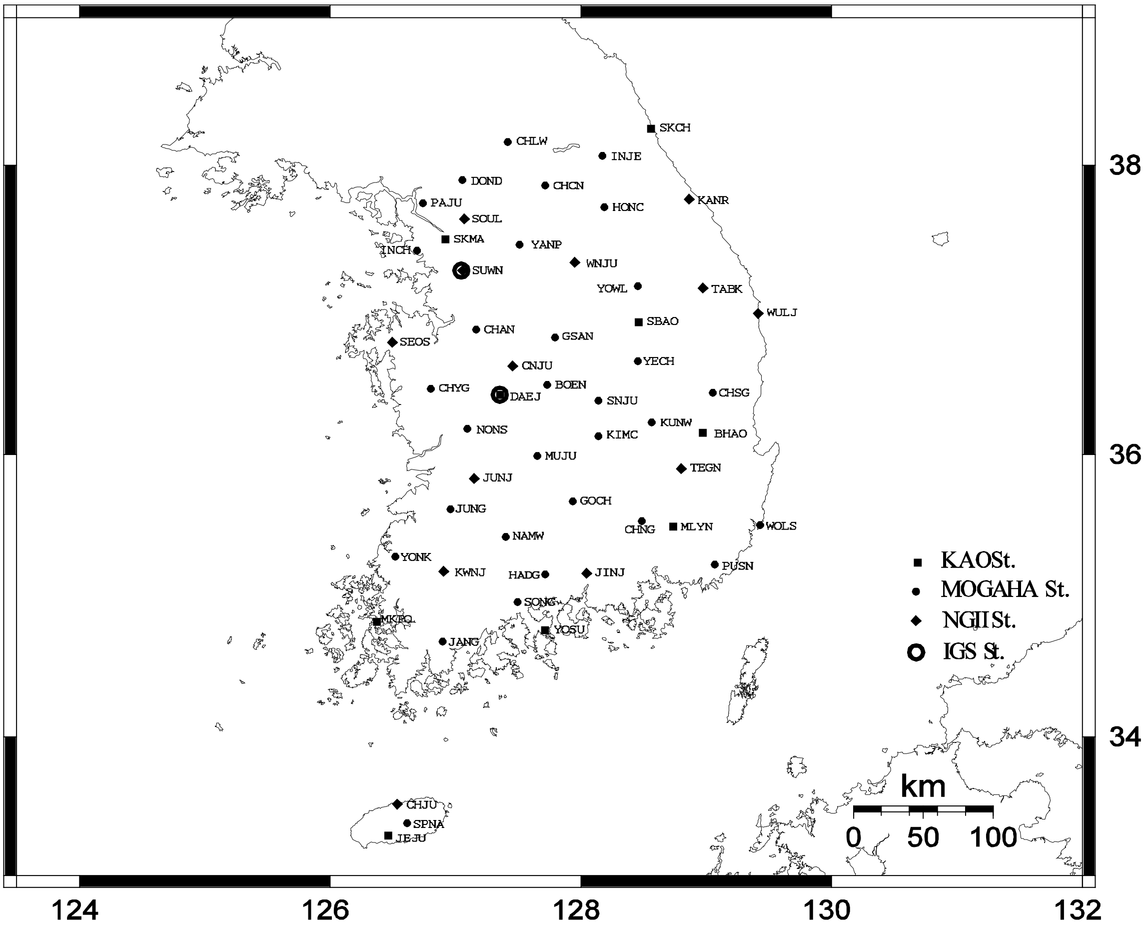

Fig. (1): Korean GPS Network (KGN) and its constellation.

<u>http://www.ngs.noaa.gov/ANTCAL/Models/TRM_choice.html</u>. Also we use the constrained network adjustment technique (where DAEJ station considered to be fixed) in the adjustment step to eliminate the effect of the common-mode signal in the daily vertical velocity. Finally we unify the reference system for all the solutions where all the stations coordinates and velocities calculated in the ITRF97. This is done in-order to avoid any jumps in the velocities time series. The used adjustment technique not only eliminates the effect of common-mode signal but also it eliminates the effect of the periodic phenomena. The weekly solutions are created by combine the daily normal equations using the ADDNEQ program. The stations vertical velocities are estimated by least squares linear fitting for the changes in station position (normal component) with respect to time. They are listed with their RMS errors in Table 2 and examples of the time series are represented in Figure 2.

DISCUSSION

Formally, the GPS rates refer to the Earth's center of mass, and levelling refer to the Geoid and they can be correlated by the equation ($\Delta H = \Delta h + \Delta N$) *where, ΔH is the change in ellipsoidal height, Δh is the change in orthmetric height and ΔN is the change in Geoidal undulation.* From this equation it is clear that the Normal velocities, which depicted from the GPS include the changes in undulation (ΔN) during the considered time. Ekman and Mäkinen , 1996 estimated that the vertical velocities depicted by GPS are considered to be 4-7% larger than the levelled rates.

The processing method raises two concerns. First, we reduce the variation in the common-mode signals by using the antenna phase center correction for all the used antenna types. Secondly, we minimize the effect of common-mode signals in the depicted velocities by keeping DAEJ station fixed and calculating the vertical velocity with respect to it. Using the resulted station's vertical velocities (Table 2) a contour map for the vertical movement in the Korean peninsula, with an interval of 0.5mm/yr, were plotted (Fig. 3). Throughout this map it is clear that the maximum velocity is less than 3mm/yr while the average one is 1.3mm/yr. There are some gaps in this map, especially in the western part of the study area, resulted from the exclusion of six station velocities because of their relatively high RMS.

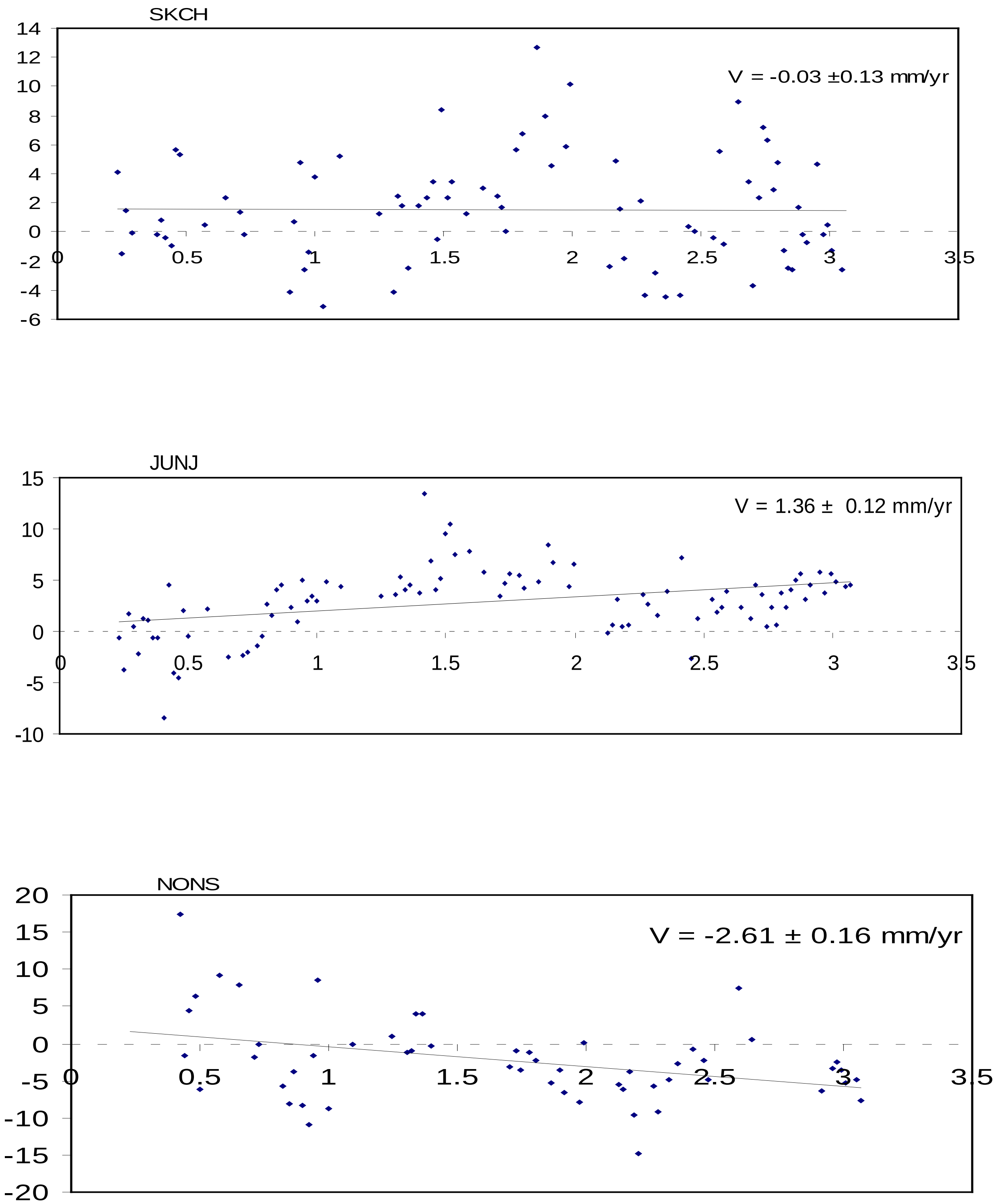

Fig. (2): Examples of the normal velocity time series depicted from the KGN.

SKCH is a KAO site
JUNJ is a NGII site
NONS is a MOGAHA site

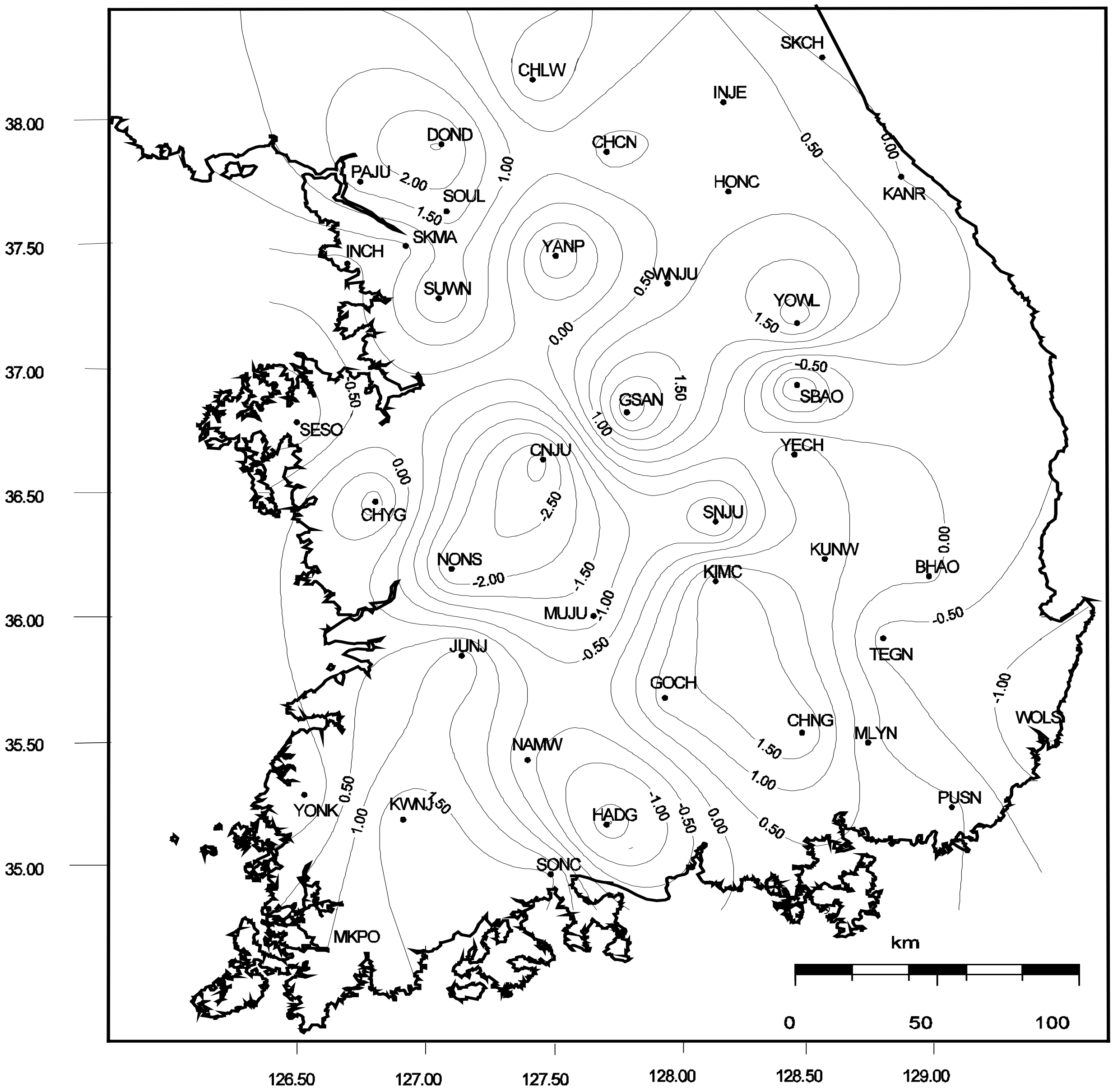

Fig. (3): Contour map for the vertical movement in the Korean peninsula

In spite of the fact that our GPS results represent the velocity rate in the upcomponent (with respect the Earth's center of mass) but it gives reliable information about the vertical movements in the Korean peninsula in the absence of repeated precise levelling data.

CONCLUSION

The previous discussion helps to conclude that the antenna phase center correction eliminates the variation in the common-mode signals found in the time series of the KGN station's velocity (this variation results from the use of different antenna types), while the effect of common-mode signals can be minimized by using the fixed network adjustment technique.

The maximum depicted vertical velocity in the Southern part of the Korean Peninsula is 3 mm/yr while the average one is 1.3 mm/yr.

Unfortunately, our results can't be compared with any other source of vertical movements detection methods (levelling and/or tide gauges) but we believe that our results (*ΔH which obtained from GPS*) give reliable information about the vertical movements in Korea.

The more time we have the more accurate velocity we can obtain and it is recommended to investigate the effect of the environmental condition in each of the KGN stations in order to have much more accurate vertical velocities.

ACKNOWLEDGMENT

The author thanks the GPS team in the Korea Astronomy Observatory for their helpful discussion. I am so grateful for the National Geographic Information Institute of Korea and the Ministry of Government Administration and Home Affairs for contributing their data. This work was supported by the Korean Ministry of Science and Technology via grant M20313010001-03A0213-00410.

REFERENCES

Beutler, D. F., et al., 2001, Bernese *GPS software Version 4.2*, Astronomical Institute, University of Bern.

Cho H., 1999, Grids and Datum the Republic of Korea. Journal of the American Society for Photogrammetry and Remote Sensing, Vol. 65, N11 Pp. 1243-1247.

Park Pil-Ho., Chwa U., Ahn Y. and Choi K., 2001, Preliminary GPS results and a possible neotectonic interpretation for the South Korea. Earth Planets Space, 53. 973-942.

Park Pil-Ho, Kwan-D Park, Hamdy A. M. and Lim H., 2003, AGU fall meeting, G52C-0051.

Hamdy A.M., Park Pil-Ho., Kwan-D Park, and Lim H., 2004, Prelimanry results from the Korean GPS Network. Submitted to Geosciences journal.

Mäkinen J., Koivula H., Poutanen M. and Saaranen V., 2003, Vertical velocities in Finland from GPS networks and from repeated precise levelling, Journal of Geodynmics, Vol. 38, pp. 443-456.

Mao, A., Harrison, C.G.A. and Dixon, T.H., 1999, Noises in GSP coordinate time series. J. Geophys., Res. 104, 2797-2816.

Scherneck H.-G., Johansson J. M., Elgered G., Davis J. L., Jonsson B., Hedling, G., Koivula H., Ollikainen M., Postanen M., Mitrovica J.X. and Milne, G.A., 2002, BIFROST: Observing the three-dimensional deformation of Fennoscandia. In: Mitrovica J.X., Vermeersen B.L.A. (Eds), Ice sheets, Sea level and Dynamic Earth, AUG Geodynamics Series, Vol. 29. AUG, Washington, DC, pp. 69-93.

Egyptian Geophysical Society
EGS Journal, vol. 3, No. 1, 41-48 (2005)

THREE-DIMENSIONAL P-AND S-WAVES VELOCITY STRUCTURE BENEATH THE NORTHERN PART OF THE ASWAN HIGH DAM LAKE AREA

Abu Bakr A. Shater

National Research Institute of Astronomy and Geophysics

دراسة تراكيب سرعة الموجات الابتدائية والثانوية فى الأبعاد الثلاثة لمنطقه شمال بحيرة السد العالي بأسوان

الخلاصة: تناول البحث دراسة تراكيب سرعة الموجات الابتدائية (P-wave) والثانوية (S-wave) في الأبعاد الثلاثة لمنطقه شمال بحيرة السد العالي بأسوان وذلك باستخدام الزلازل المحلية والمسجلة بواسطة المحطات السيزمية لشبكة الزلازل بأسوان. و أظهرت النتائج أن الجزء الغربي لبحيرة السد العالي وهى منطقه وجود الفوالق تتميز بوجود سرعات منخفضة للموجات الابتدائية وتمتد هذه المنطقة إلى أسفل حتى تصل الى عمق ١٢ كيلو متر بينما توجد منطقه للسرعات العالية للموجات الابتدائية فى الجزء الجنوبي الشرقي لمنطقه الدراسة وتمتد أفقيا تجاه الجنوب الغربي وإلى أسفل متجها إلى الغرب حتى عمق ١٩ كيلو متراً كما تظهر منطقه لسرعات منخفضة للموجات الابتدائية في الجزء الشرقي على عمق ٦ كيلومترات وتمتد أفقيا تجاه الجنوب الغربي وإلى اسفل حتى عمق ١٩ كيلو متر.

أما بالنسبة للموجات الثانوية فمنطقة وجود الفوالق فى الجزء الغربي لبحيرة السد العالى تتميز أيضا بوجود سرعات منخفضة للموجات الثانوية وتمتد هذه المنطقة الى اسفل حتى تصل إلى عمق ١٢ كيلومتر، كما تظهر منطقه للسرعات العالية للموجات الثانوية فى الجزء الشرقي لمنطقه الدراسة وتمتد أفقيا تجاه الجنوب الغربي وإلى أسفل حتى عمق ٦ كيلومترات.

ABSTRACT: *The estimation of three-dimensional velocity structure under the northern part of the Aswan High Dam Lake region was achieved. This implied the application of inversion of the P-wave and S-wave arrival times from the local earthquakes occurring under Aswan Seismic Network area.*

The final crustal velocity model features a low P-wave velocity trend along the faults region in the western side of the Aswan High Dam Lake extended down to 12 km. A high velocity block appears in the southeast of the studied area at depth 2 km and extended down to 19 km trending to west direction. Low P-wave velocity zone appears at depth 6 km in the eastern side and extended down to 19 km trending toward the center of the region.

Low S-wave velocity was found in the western side under Gabal Marrawa (GMR) station on the Kalabsha fault region extended horizontally to northeast and down to 19 km. High S-wave velocity appears in the north eastern side of the Aswan High Dam Lake at depth 2 km extended horizontally to southwest direction and down to 6 km.

INTRODUCTION

The Aswan High Dam was constructed in the southern part of Egypt on the Nile River, The water of the Nile River is impounded in the Nasser Lake. A seismographic telemetered network was installed at the northern part of Aswan Reservoir by the National Research Institute of Astronomy and Geophysics and Lamont Doherty Geological Observatory of Colombia University. The purpose of the network is to monitor induced seismic activity, along the Kalabsha fault, which continues to occur in the area since the earthquake of November 14, 1981 with magnitude 5.5. (Kebeasy et al. 1982 and 1987). The pattern of seismicity in the Aswan area suggests that a transition zone lies between the higher level of seismicity within the Red Sea or along the Red Sea border to the lower level of seismicity west of the Nile valley in the desert.(Woodward Clyde report, 1985).

The purpose of this study is to image the 3-D seismic velocity structure beneath the Aswan High Dam Lake region. The data was obtained from Aswan Seismic Network. It consists of 13 remote stations distributed around the northern part of the Aswan High Dam Lake, 11 of them are distributed around the active faults in the area. They are located at the western side of the lake while the rest of them are located at the eastern side. They are mainly used to control the extension of the E-W Kalabsha active fault. Data acquisition and analysis were carried out in the center located at Aswan Seismological Data Center, (Figure 1 and table 1). The arrival times were measured as a part of routine processing of Aswan Seismological Data Center. The hypocenter location and the origin time of an earthquake were determined by using the HYPO71PC program (Lee and Lahr, 1994).

Figure (2) Location map

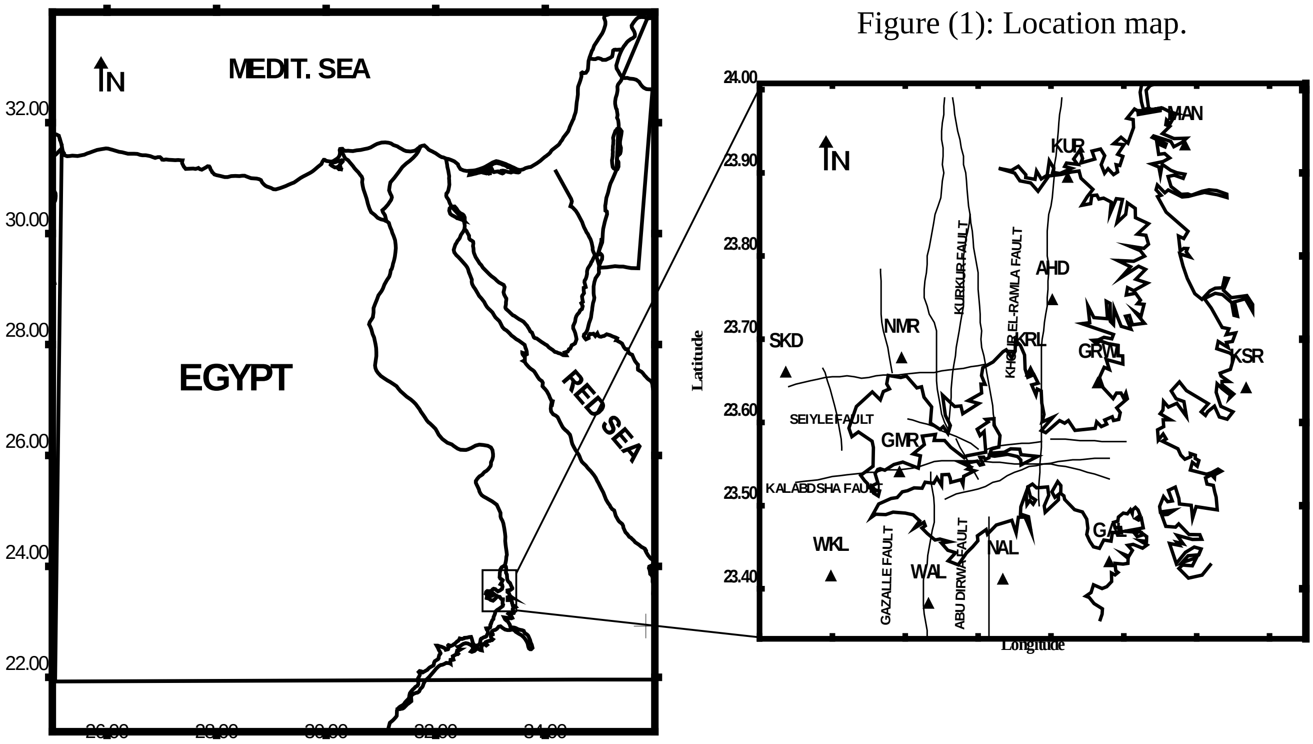

Figure (1): Location map.

Table (2) P-wave crustal velocity strucutre

Layer (Km)	P-wave velocity (Km/s)	Thikness (Km)
1	5.168	3.825
2	6.202	10.120
3	7.02	16.064
4	8.01	

Table (1) Aswan seismic network stations

Number	Station	Latitude	Longitude	Elevation
1	KSR	23.642	33.018	230
2	KUR	23.895	32.773	190
3	MAN	23.934	32.934	245
4	WAL	23.383	32.582	197
5	AHD	23.748	32.752	222
6	SKD	23.661	32.386	270
7	NMR	23.678	32.545	200
8	GMR	23.541	32.542	270
9	WKL	23.416	32.448	203
10	GAL	23.433	32.83	278
11	KRL	23.662	32.722	185
12	NAL	23.412	32.684	200
13	GRW	23.648	32.814	260

MATERIAL AND METHOD

P- and S- arrival times recorded at the Aswan Seismic Network were used to perform nonlinear optimization for velocity and hypocenters, and to perform linearized inversion in the Aswan High Dam Lake region. We recorded and timed a total of 393 P-wave arrivals and 393 S-wave arrivals at 13 network stations from 178 events. The maximum number of arrival time picks per event is 13.

The initial velocity model is the laterally homogeneous model used by Aswan Seismic Network, for routine hypocentral locations as shown in table (2). The results of routine work processing were used as initial hypocenteral coordinates and origin times.

The program SIMULPS was used for this study; this was originally developed by Thurber (1983 and 1993) using approximate ray tracing (ART) and pseudo-bending (PB) algorithms and further improved by Eberhart-Phillips (1990 and 1993), for forward modeling of P- and S-wave arrival times in an iterative, damped, least-squares inversion for hypocenters and three-dimensional velocity structure. The method also employs the parameter separation technique (Pavlis and Booker, 1980; Spencer and Gubbins, 1980) which allows to computationally split the problem into two, e.g., solving for the hypocenters and velocity model separately, while maintaining the mathematically coupled nature of the overall problem. Evans et al., (1994) described in detail the technique and all the parameters involved. (Hauksson and Haase, 1997).

The residuals can be related to the desired perturbations to the hypocenters and velocity structure parameters by a linear approximation. The unknown hypocenter location parameters are also one of the limits of integration of the last term in the following equation which has the same formula for P- and S- arrival times data.

$$rij = \sum_{k=1}^{3} \frac{\partial \mathrm{T}ij}{\partial \mathrm{X}k} \Delta \mathrm{X}k + \Delta t + \sum_{i=1}^{l} \frac{\partial \mathrm{T}ij}{\partial mi} \Delta mi \qquad (1)$$

where m_1 represents the parameters of the velocity model. The velocity model partial derivatives $\partial T_{ij}/\partial m_i$ are essentially line integrals along the raypath reflecting the relative influence of each model parameters on a given travel time datum.

Velocity model parameterizations for the linearized inversion used a 10 (x) by 9 (y) by 4 (z) grid of nodes with a node spacing of 6 km in the X axis and 7 km in the Y axis.

RESULTS

The results obtained from a three- dimensional inversion of the local P-wave and S-wave travel time data are following the method in the preceding section. The P-wave and S-wave velocity values (upper number) with velocity perturbation (lower number) in each depth are shown as a final model in Fig. (2). In this figure, areas with negative velocity perturbations are marked "L", and areas with positive velocity perturbations are marked "H". Figure (3) shows the result of the inversion in black and white plots as follows:

P-wave velocity structure at the top layer (depth range 0-2 km, Fig 3 a) is dominated by high velocity zone under Khour Sakr (KSR) seismic station in the eastern bank of the Aswan High Dam Lake trending to south-west direction. Low velocity zone appears under North Marrawa (NMR) and Gabal Marrawa (GMR) stations in the western part along the faults region trending to north-south and low velocity zone appears in the north-eastern part of the Lake under Manam (MAN) seismic station that is trending to south- west direction. Low velocity zone appears also in the southern part of the Lake under Gabal Alisa (GAL) seismic station. High velocity zone trending to west direction appears under the middle of northern part of the Lake under Abu hadid (AHD) station.

S -wave velocity structure at the same layer (depth range 0-2 km, Fig 3 b) is dominated by high velocity zone in the north of Khour Sakr (KSR) seismic station in the eastern bank of the Aswan High Dam Lake trending to south-west direction and high velocity zone appears in the west of the Gabal Marrawa (GMR) station trending to north-east direction. Low velocity zone appears in the north-eastern part of the Aswan High Dam Lake under Manam (MAN) seismic station trending to south- west direction. Also low velocity zone appears in the southern part of the Aswan High Dam Lake under Gabal Alisa (GAL) seismic station trending to north-east direction.

The overall pattern of P-wave velocity perturbation in layer 2 (depth range 2-6 km Fig. 3 c), exhibits high velocity zone appears in the north-eastern side of the Aswan High Dam Lake under Manam (MAN) seismic station extended horizontally to southwest direction and sandwiched by two low velocity zones. Low velocity zone appears under Gabal Marrawa (GMR) station. High velocity zone appears under Khour Sakr (KSR) station extended horizontally to southwest direction

Fig. (2): P-wave and S-wave velocity values (upper numbers) and velocity pertrubations (lower numbers).

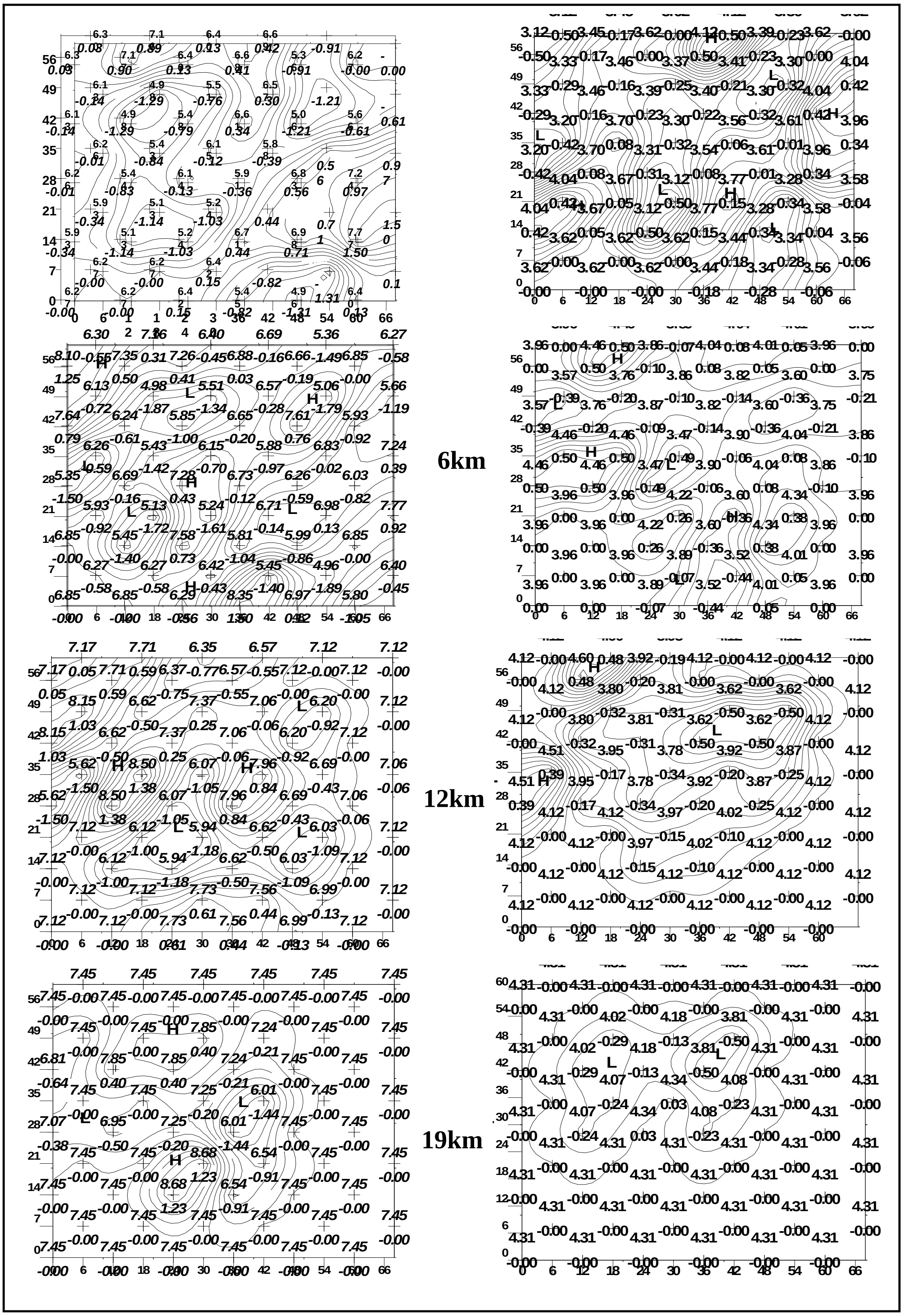

Fig. (3):P-wave and S-wave velocity contour lines in different depths.

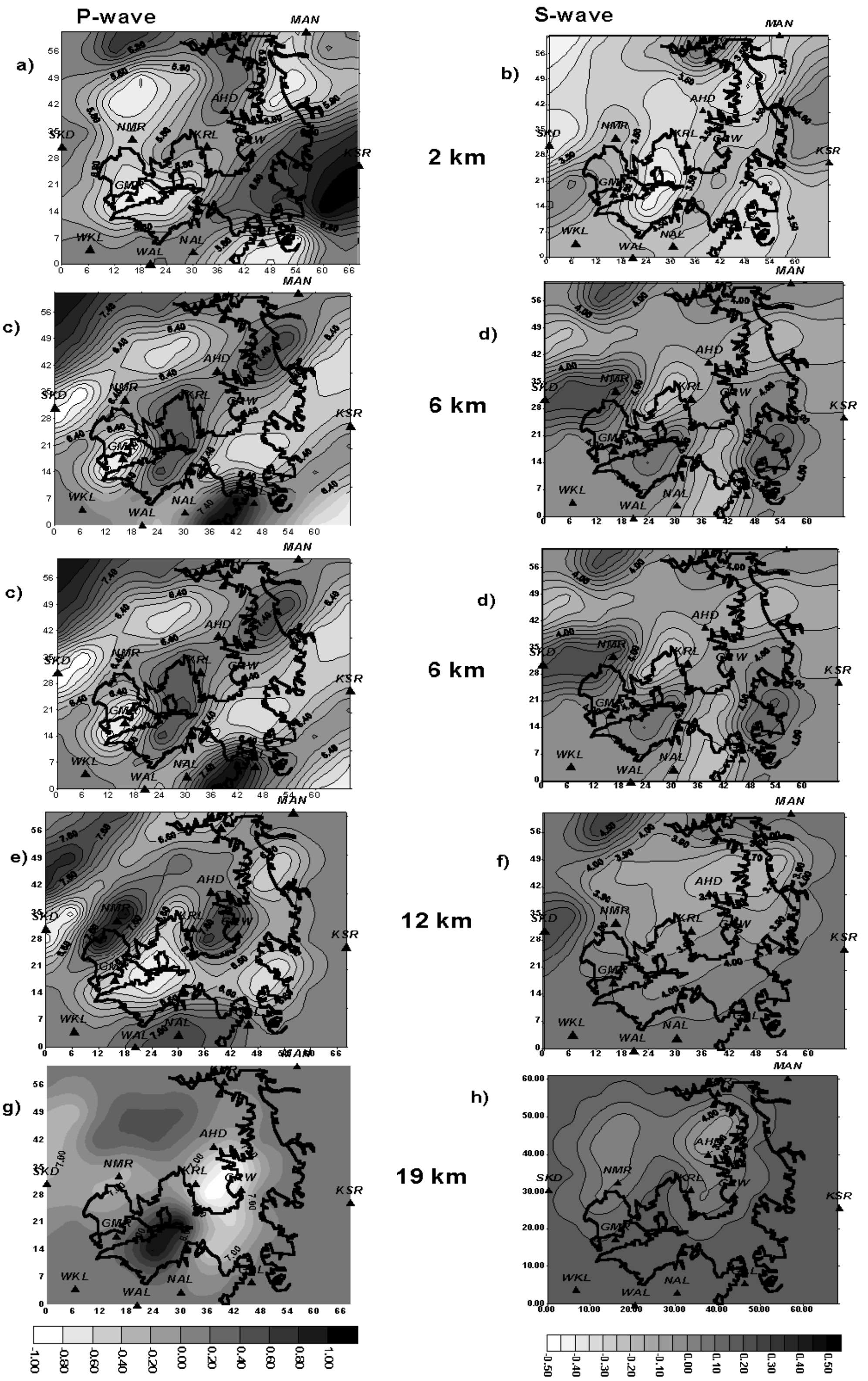

Fig. (4):Final model of 3-D inversion for (a) P-wave and (b) S-wave.

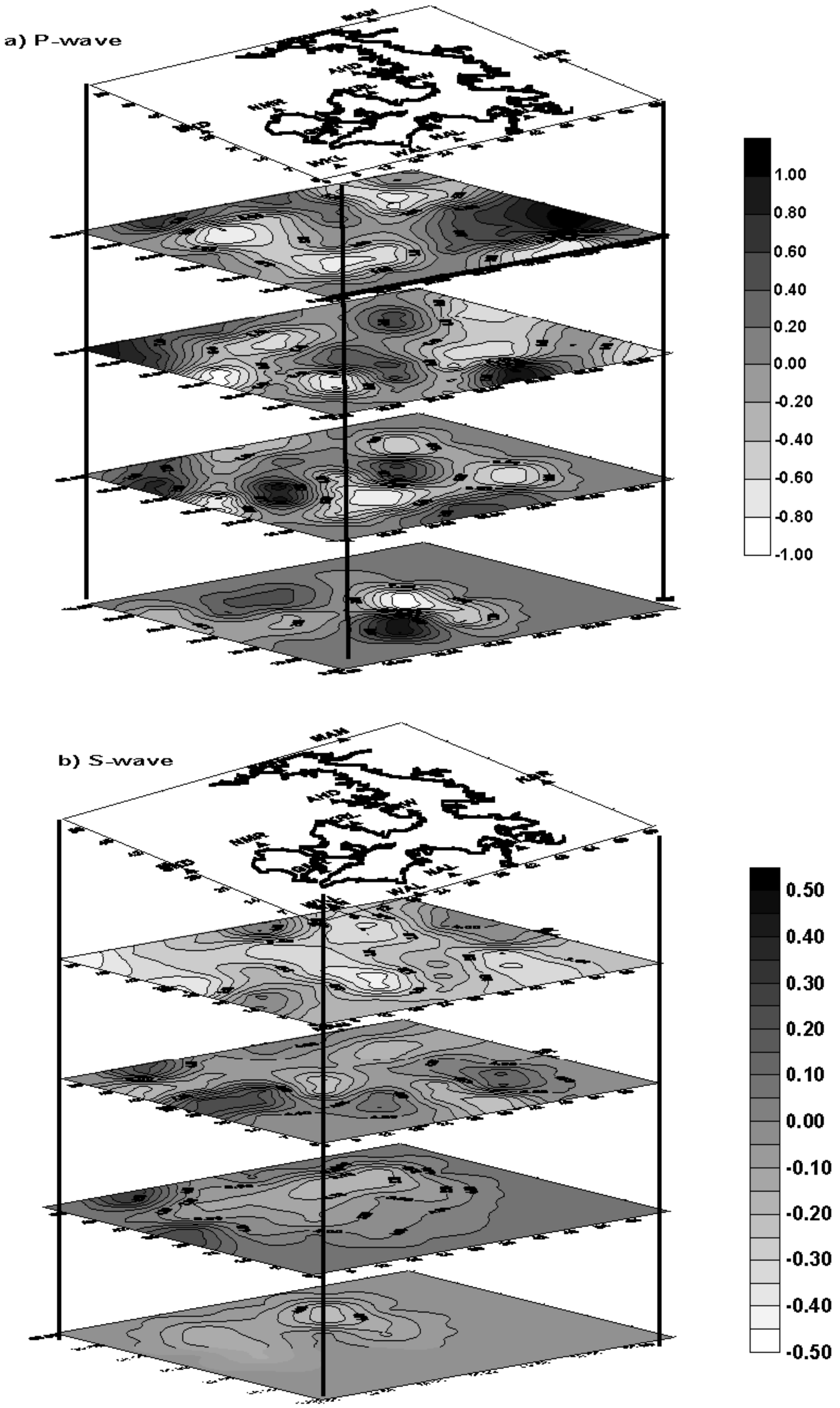

S-wave velocity structure relevant to this layer (Fig 3 d) exhibits high velocity zone under Kurkur (KUR) and Abu Hadid (AHD) seismic stations extended horizontally to west direction. Also, high velocity zone appears under Sinn el Kaddab (SKD) seismic station extended horizontally to northeast direction. Low velocity zone appears between new alisa (NAL) and Gabal Alisa (GAL) seismic stations extended horizontally to northeast and northwest directions and it is bounded by two high velocity zones from the east and west.

Third layer at the depth range 6 -12 km (Fig. 3 e), illustrates, a high velocity zone appears near the center of the studied area under Abu Hadid (AHD), Khour Ramla (KRL) and Gabal Rawraw (GRW) stations and bounded by two low velocity zones from the east and west. Low velocity zone appears under Sinn el Kaddab (SKD) station extended to northeast direction. High velocity zone appears under North Marrawa (NMR) and New Alisa (NAL) seismic stations.

S-wave velocity structure at this layer (Fig. 3 f) demonstrates a low velocity zone under Abu Hadid (AHD) station which decreases outward to west and southwest directions. High velocity zone appears under Sinn el Kaddab (SKD) station extended to northeast direction.

Layer 4 at depth range 12-19 km, (Fig. 3 g) is characterized by a low velocity zone appears near the center of the studied area between Abu Hadid (AHD), Khour Ramla (KRL) and Gabal Rawraw (GRW) stations and extended horizontally to west under North Marrawa (NMR) station and to south direction, meanwhile the two high velocity zones are located in the north and south of the North Marrawa (NMR) station.

S-wave velocity structure at this layer (Fig. 3 h) is characterized by a low velocity zone in the west bank of the lake under Abu Hadid (AHD) and North Marrawa (NMR) seismic stations.

Figure (4) shows the final model of three-dimensional velocity structure under the northern part of the Aswan High Dam Lake region. The thick line represents the smoothed boundary between positive and negative pertrubation values.

CONCLUSION

In the present study, tomographic inversion is applied to cover 61x 68x 19 km region in the northern part of the Aswan High Dam Lake. Grid parameterization is adopted in the studied area. The grid points were distributed at every 6 km in X direction and 7 km in Y direction at depths 2, 6, 12 and 19 km. About 393 P-wave and 393 S-wave arrival times recorded at 13 seismic stations from well located earthquakes were used in the inversion.

The final crustal velocity model features a low P-wave velocity trend along the faults region in the western side of the Aswan High Dam Lake extended down to 12 km. A high velocity block trending to west direction appear in the southeast of the studied area at depth 2 km and extended down to 19 km. Low P-wave velocity zone appears at depth 6 km in the eastern side and extended down to 19 km. It is trending toward the center of the region.

Low S-wave velocity was found in the western side under Gabal Marrawa (GMR) station on the Kalabsha fault region extended horizontally to northeast and extended down to 19 km. High S-wave velocity appears in the north eastern side of the Aswan high Dam Lake at depth 2 km extended horizontally to southwest direction and down to 6 km..

ACKNOWLEDGMENT

I would like to express my sincere gratitude and appreciation to Prof. E. M. Ibrahim , Prof.. R. M. Kebeasy and Prof. R. N. Albert for their help. I also wish to extend my thanks to Prof. M. A. El-Hefnawy and all Aswan Seismic Observatory staff.

REFERENCES

Eberhart-Phillips, D. (1990). Three-dimensional P- and S- velocity structure in the Coalinga region, California, J. Geophys. Res. **95**, 15343-15363.

Eberhart-Phillips, D. (1993). Local earthquake tomography: earthquake source regions, in Seismic Tomography: theory and practice, ed. Iyer, H. M, and K. Hirahara, 613-643, Chapman and Hall, London.

Evans, J. R., D. Eberhart-Phillips, and C. H. Thurber (1994). User's manual for SIMULPS12 for imaging Vp and Vp/Vs: A derivative of the ``Thurber" tomographic inversion SIMUL3 for local earthquakes and explosions, U.S. Geol. Surv. Open File Rep. **94-431**, 101p.

Hauksson, E., and J. S. Haase (1997). Three-dimensional Vp and Vp/Vs velocity models of the Los Angeles basin and central Transverse Ranges, California, J. Geophys. Res. **102**, 5423-5453.

Kebeasy, R., Maamoun M., Ibrahim E., Mogahed A.,W. Simpson D., and Leith W. (1987) : Earthquake studies at Aswan Reservoir. Journal of Geodynamics, vol. 7, p. 173-193.

Kebeasy, R. , Maamoun M., and Ibrahim, E., (1982) : Aswan Lake Induced Earthquakes, Bull. International Inst. of Seismology and Earthquake Engineering, Vol. 19, 1982, Tokyo.

Lee , W.H.K. and Lahr, J.C., (1994) : Toolbox for seismic processing, and analysis, IASPI software Library, Volume 5, P.O. Box "I" Menlo Park, CA 94026, U. U.S.A., PP 207.

Spencer, C., and D. Gubbins (1980). Travel time inversion for simultaneous earthquake location and velocity structure determination in laterally varying media, Geophys. J. R. Astron. Soc. 63, 95-116.

Pavlis, G. L., and J. R. Booker (1980). The mixed discrete-continuous inverse problem: Application to the simultaneous determination of earthquake hypocenters and velocity structure, J. Geophys. Res. **85**, 4801-4810.

Thurber, C. H. (1983). Earthquake locations and three-dimensional crustal structure in the Coyote Lake area, central California, J. Geophys. Res. 88, 8226-8236.

Thurber, C. H. (1993). Local earthquake tomography: velocities and Vp/Vs - theory, in Seismic Tomography: theory and practice, ed. Iyer, H. M, and K. Hirahara, pp. 563-583, Chapman and Hall, London.

Woodward-Clyde Consultants, (1985): Aswan High Dam Seismic Project, a report submitted to High Dam and Aswan Dam Authority (HADA), Subtask 1 E.